Scientific paper

Photoinduced Tautomerism of 2-Thiobarbituric Acid Studied by Theoretical and Experimental Methods

Rumyana I. Bakalska and Vassil B. Delchev*

Faculty of Chemistry, University of Plovdiv, BG-4000 Plovdiv, Tzar Assen 24 Str., Bulgaria

** Corresponding author: E-mail: vdelchev@uni-plovdiv.bg*

Received: 10-03-2011

Abstract

Combined, theoretical and experimental, investigation was performed to study the mechanism of the photoinduced tautomerism of 2-thiobarbituric acid (TBA). The irradiation of the solution of TBA in polar aprotic solvent with UV light (maximum at 366 nm) showed oxo–hydroxy photoisomerization of the triketo form of TBA to the hydroxy-imino tautomer. The studied mechanisms (TD DFT) of the photoinduced NH and OH dissociations in the keto and enol tautomer revealed that the proton detachment in the triketo tautomer occurs in the bright $^1n_S\sigma^*$ excited state. In the hydroxy-imino tautomer this mechanism is driven by the repulsive $^1\pi\sigma^*$ excited state. The excited-state relaxation mechanisms occur by low-lying S_o–S_1 conical intersections.

Keywords: Conical intersections, photochemistry, proton detachment, TD DFT calculations, 2-thiobarbituric acid, UV irradiation

1. Introduction

Thiobarbituric acid (TBA) is a sulfur derivative of barbituric acid in which the oxygen atom at the second position is replaced by a sulfur atom. Being analogue of barbituric acid, TBA shows significant difference in the enolization tendency as well as in the spectral features.[1] The interest in barbiturates is provoked by the fact that they were in therapeutic use as CNS depressants (sedation, hypnotic, preanaesthetic, anticonvulsant activity, headache products etc.) for a long time.[2] Barbiturates are strongly electron-withdrawing because they gain aromatic stabilization upon reduction.[3] This property has been exploited in the preparation of molecules which possess pronounced quadratic non-linear optical properties – of interest for potential applications in optoelectronic and photonic technologies.[4,5]

TBA is an object of a large number of investigations. As concerns the spectroscopic features of this compound, Mendez et al have identified one intense UV band of this compound in methanol solution at 283 nm with a well-defined shoulder at 265 nm.[6] They have discussed also the nature of the two less intensive absorption bands at 244 and 227 nm. Further, the analysis of the vibration spectrum of TBA in the solid state has demonstrated that the compound exists in two tautomeric forms in equal amounts: the triketo tautomer of TBA and one enol tautomer.[6,7] This is the enol tautomer with a CH group at the fifth position. The same enol form of TBA has been found by Goel in the solid state of TBA.[8] In solvents with a large dielectric constant the enol tautomer predominates.[9] Zuccarello et al have performed a detailed study of the tautomeric equilibria in TBA.[1] They have discussed the presence of neutral tautomers as well as their anions and protonated forms in water solution at different pH. However, no comment has been done for the potential possibility of TBA to phototautomerize upon UV-irradiation.

Millefiori et al have studied theoretically (at the semiempirical level AM1) the possible tautomers of thiobarbituric acid.[10] They have found, in agreement with the experiment, that the barbiturate ring is essentially planar.[10] The investigation of Chierotti et al reports about the possibility of the enol and keto tautomers of TBA to participate in intermolecular H-bonding and thus to form large clusters.[7] Both forms are stable and form polymorphous crystals at different conditions.

Martos-Calvente et al have discussed the usefulness and accuracy of the DFT theory for description of the tautomeric equilibria thienol–thione.[11] They have found that the calculated vibration spectra of the model compounds fit fairly well with the experimental IR spectra. Moreover,

DFT calculations interpret rather accurately the SH stretching vibration.[11]

The purpose of the current research is to throw light upon the mechanism of photoinduced tautomerism of TBA. Several theoretical studies have revealed that in the most cases (e.g. pyrimidine derivatives) this mechanism is connected to the dissociation of the proton and subsequent association to another atom (O, C etc.) by the so-called PIDA mechanism (photoinduced dissociation-association).[12–14] It is believed (for pyrimidine bases) that this mechanism is driven by the repulsive $^1\pi\sigma^*$ excited state.[12,13]

2. Computational Methods

All tautomeric forms of TBA were optimized at the TD DFT (B3LYP) and CC2 theoretical levels (CC2-resulted geometries are given in ESI). Subsequent frequency calculations were performed to prove that the molecules are located in real minima.

The B3LYP-optimized geometries of the ground states of the tautomers were used for subsequent calculations of the vertical excitation energies of the singlet electronic states. The obtained vertical excitation energies were compared to the experimental UV bands (recorded in acetonitrile) of non-irradiated and irradiated samples of TBA.

All calculations were performed with the aug-cc-pVDZ basis functions and the program packages GAUSSIAN 03, and TURBOMOLE (for the CC2-calculations given in ESI) with C_S symmetry restrictions.[15–19]

3. Experimental Methods

2-Thiobarbituric acid (anhydrous) was purchased from Fluka and acetonitrile was from Lab-Scan (super gradient).

Photochemical irradiations were carried out in a standard Pyrex immersion reaction vessel. As a UV-light source we used a high pressure mercury lamp TQ 150 with Quartz filter (Heraeus Noblelight, Germany).

The solution (0.0606 g of 2-thiobarbituric acid in 250 mL acetonitrile) was deoxygenated with nitrogen (30 min). Nitrogen was bubbled trough the solution during the irradiation (1 h). The course of the reaction was followed by UV-spectroscopy at every 10 min. The UV spectra were recorded with a Cintra 101 UV/VIS spectrophotometer.

The IR-spectra of irradiated and non-irradiated samples were recorded with VERTEX 70 FT-IR spectrometer (Bruker Optics) as KBr discs. For the preparation of the KBr disc, acetonitrile of the part of irradiated sample (10 mL) was insufflated with nitrogen under vacuum in a closed vessel without heating. The contact of the irradiated solution with oxygen (air) caused oxi-reduction process and elementary sulfur is produced quickly.

4. Results and Discussion

4. 1. Ground-State Equilibrium Geometries of the Tautomers

The ground-state equilibrium geometries of several tautomeric forms of TBA were optimized at the B3LYP/aug-cc-pVDZ level. They are illustrated in Fig. 1 and several structural parameters are listed in Table 1.

We chose the tautomers (E, E1, E2) that can be formed directly from the triketo form and two extra tautomers which can be obtained by tautomer E1 (E3 and E4). In this way, we comprised all kind of proton transfer mechanisms in TBA: and C···H···O, S···H···N, O···H···N. Moreover, the IR spectra of irradiated TBA were informative enough to help decide which tautomers to take into consideration in the present study.

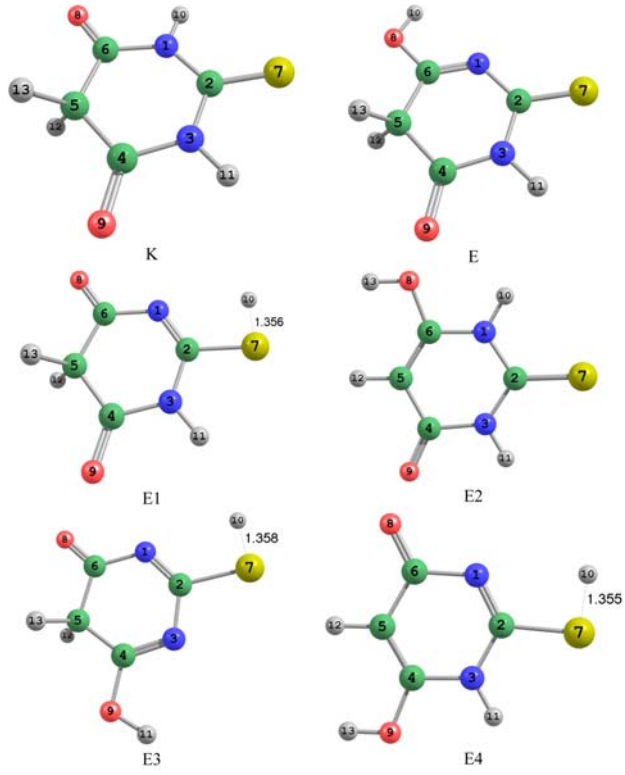

Figure 1. Optimized structures of the tautomeric forms of 2-thiobarbituric acid.

In agreement with previous investigations,[7,10] the data in Table 1 show that all tautomers are planar. In the tautomers K, E, E1 and E3 the CH_2 hydrogens are symmetrically located with respect to the molecular plane. The presence of a symmetry plane facilitates the assignment of the molecular orbitals and the electronic excited states by symmetry. By the symmetry rules, we classified the molecular orbitals in two groups: with symmetry a' – n_o / n_N / σ-MO; and with symmetry a'' – π-MO. Therefore, the electronic excited states were divided into two

Table 1. Selected structural parameters of the tautomers of TBA

Paramater	K	E	E1	E2	E3	E4
$r(N_1C_2)$ *	1.378	1.387	1.290	1.380	1.298	1.284
$r(C_2N_3)$	1.379	1.395	1.383	1.366	1.399	1.380
$r(N_3C_4)$	1.394	1.383	1.397	1.420	1.289	1.376
$r(C_4C_5)$	1.514	1.515	1.510	1.449	1.491	1.355
$r(C_5C_6)$	1.514	1.497	1.532	1.361	1.534	1.465
$r(N_1C_6)$	1.394	1.287	1.404	1.373	1.396	1.424
$r(C_4O_9)$	1.215	1.217	1.213	1.222	1.335	1.354
$r(C_6O_8)$	1.214	1.338	1.214	1.348	1.215	1.222
$r(C_2S_7)$	1.660	1.656	1.778	1.669	1.766	1.789
$\theta(N_1C_2N_3C_4)$ **	0.0	0.0	0.0	0.0	0.0	0.0
$\theta(C_2N_3C_4C_5)$	0.0	0.0	0.0	0.0	0.0	0.0
$\theta(N_3C_4C_5C_6)$	0.0	0.0	0.0	0.0	0.0	0.0
$\theta(C_4C_5C_6N_1)$	0.0	0.0	0.0	0.0	0.0	0.0
$\theta(C_5C_6N_1C_2)$	0.0	0.0	0.0	0.0	0.0	0.0
$\theta(H_{12}C_5C_4N_3)$	122.9	122.5	123.1	180.0	122.1	180.0
$\theta(H_{10}O_8C_6N_1)$	–	0.0	–	–	–	–
$\theta(H_{13}O_8C_6N_1)$	–	–	–	180.0	–	–
$\theta(H_{10}S_7C_2N_1)$	–	–	0.0	–	0.0	0.0
$\theta(H_{11}O_9C_4N_3)$	–	–	–	–	0.0	–
$\theta(H_{13}O_9C_4N_3)$	–	–	–	–	–	180.0

* bond lengths in Å; ** dihedral angles in deg.

groups as well: with symmetry A' – $^1\pi\pi^*$ / $^1\sigma\sigma^*$ / $^1n\sigma^*$; with symmetry A" - $^1n\pi^*$ / $^1\sigma\pi^*$ / $^1\pi\sigma^*$ etc.

4. 2. Vertical Excitation Energies and Experimental UV Maxima

The experimental UV spectrum of non-irradiated solution (in acetonitrile) of TBA shows broad bands at 280 and 228 nm. These bands agree with the UV absorption maxima of TBA in methanol which have been found by Mendez et al at 283 nm and 227 nm.[6] In order to understand the nature of the electron transitions responsible for these UV-absorption maxima we calculated, at the B3LYP level, the vertical excitation energies of the six tautomers (Fig. 1). The results are collected in Table 2.

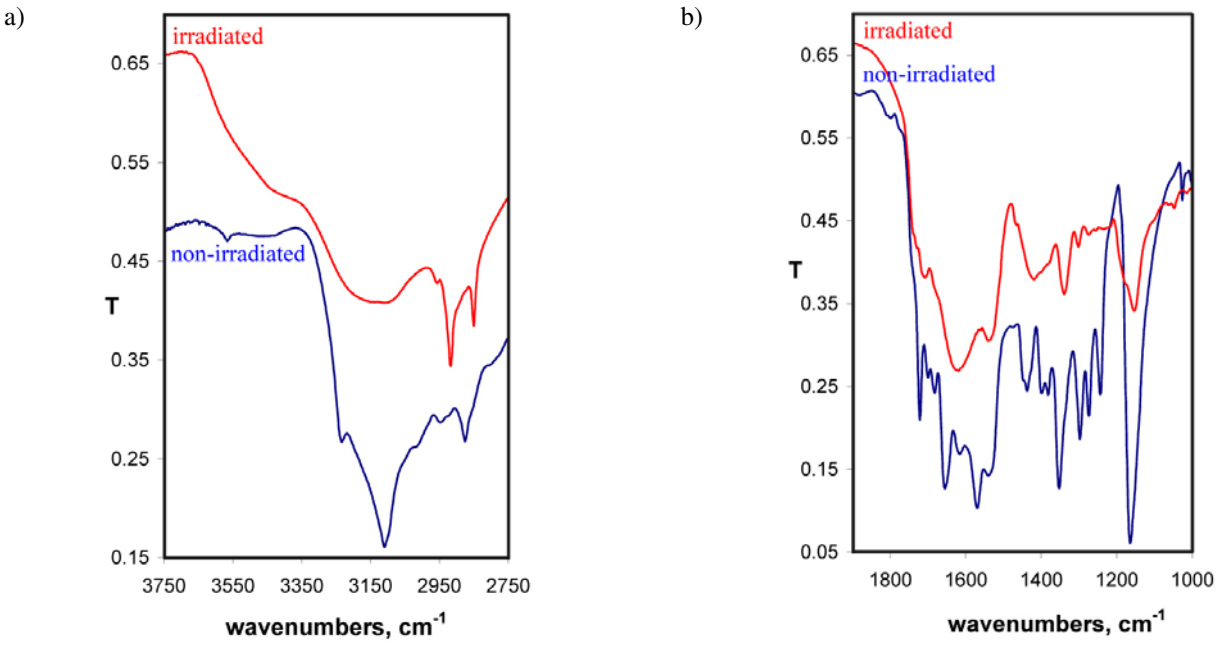

Figure 2. Selected areas (a) 3750–2750 cm^{-1}; (b) 1900–1000 cm^{-1} of the experimental IR spectra of non-irradiated (blue) and irradiated (red) TBA. The spectra were recorded in KBr discs.

Table 2. Calculated and experimental (UV, in acetonitrile) vertical excitation energies of the tautomeric forms of thiobarbituric acid

K					E				
	B3LYP		Exp.			B3LYP		Exp.	
	eV	nm	eV	nm		eV	nm	eV	nm
$^1n_S\pi^*$ (A")	3.142	395			$^1n_S\pi^*$ (A")	2.539	488		
$^1n_O\pi^*$ (A")	4.451	279			$^1\pi\pi^*$ (A')	4.373	284	4.055	306
$^1\pi\pi^*$ (A')	4.641	267	4.432	280	$^1n_O\pi^*$ (A")	4.409	281		
$^1n_O\pi^*$ (A")	4.882	254			$^1n_N\pi^*$ (A")	4.697	264		
$^1n_S\pi^*$ (A")	5.246	236			$^1n_S\pi^*$ (A")	4.805	258		
$^1\pi\pi^*$ (A')	5.454	227	5.443	228	$^1n_S\sigma^*$ (A')	5.110	243	5.065	245
$^1n_S\sigma^*$ (A')	5.513	225			$^1\pi\pi^*$ (A')	5.142	241		
$^1\pi\pi^*$ (A')	5.750	216			$^1\pi\pi^*$ (A')	5.581	222		
$^1n_S\pi^*$ (A")	5.783	214			$^1n_S\pi^*$ (A")	5.686	218		
$^1\pi\sigma^*$ (A")	5.913	209			$^1n_S\sigma^*$ (A')	5.714	217	5.881	211
E1					**E2**				
$^1n_O\pi^*$ (A")	3.713	334			$^1n_S\pi^*$ (A")	3.657	339		
$^1\sigma\pi^*$ (A")	4.568	271			$^1n_S\pi^*$ (A")	4.406	281		
$^1\pi\pi^*$ (A')	4.930	251			$^1\pi\pi^*$ (A')	4.459	278	4.432	280
$^1n_N\pi^*$ (A")	4.990	248			$^1\pi\pi^*$ (A')	4.788	259		
$^1\pi\pi^*$ (A')	5.414	229			$^1\pi\sigma^*$ (A")	4.898	253		
$^1\pi\sigma^*$ (A")	5.543	224			$^1n_S\sigma^*$ (A')	4.928	252		
$^1n_O\sigma^*$ (A')	5.622	221			$^1n_O\pi^*$ (A")	5.150	241		
$^1n_O\pi^*$ (A")	5.689	218			$^1\pi\pi^*$ (A')	5.272	235	5.443	228
$^1n_O\sigma^*$ (A')	6.233	199			$^1n_O\pi^*$ (A")	5.348	231		
$^1\pi\sigma^*$ (A")	6.263	198			$^1n_S\sigma^*$ (A')	5.494	226		
E3					**E4**				
$^1n_O\pi^*$ (A")	3.430	361			$^1n_O\pi^*$ (A")	4.417	281		
$^1n_N\pi^*$ (A")	4.159	298			$^1n_O\pi^*$ (A")	4.816	257		
$^1\pi\pi^*$ (A')	4.378	283			$^1\pi\pi^*$ (A')	5.020	247		
$^1\pi\pi^*$ (A')	5.084	244			$^1\pi\sigma^*$ (A")	5.052	245		
$^1n_N\pi^*$ (A")	5.336	232			$^1n_O\sigma^*$ (A')	5.176	240		
$^1n_O\pi^*$ (A")	5.459	227			$^1\pi\sigma^*$ (A")	5.198	239		
$^1\pi\sigma^*$ (A")	5.930	209			$^1\pi\sigma^*$ (A")	5.346	232		
$^1n_O\sigma^*$ (A')	5.931	209			$^1n_O\sigma^*$ (A')	5.355	232		
$^1\pi\sigma^*$ (A")	6.150	202			$^1\pi\pi^*$ (A')	5.531	224		
$^1\pi\pi^*$ (A')	6.212	200			$^1n_N\pi^*$ (A")	5.562	223		

Comparing the theoretical and experimental excitation energies one can say that the non-irradiated solution contains tautomer K and E2, in agreement with Ref. 6. The aforementioned bands correspond to $\pi \rightarrow \pi^*$ transitions in these tautomers. In fact the $n_S \rightarrow \sigma^*$ electron transition of the tautomer K is also included in the broad band at 228 nm (5.443 eV). It contributes to the broadening of the experimental band (the $n_S\sigma^*$ excited state is a bright state – spectroscopically active sate). The molecular orbitals involved in the electronic transitions are illustrated in the supplementary information (ESI).

The calculated vertical excitation energies of the low-lying dark $^1n_S\pi^*$ excited states are rather small. The reason might be the large diffuseness of the electron density of the sulfur atom as compared to the oxygen atom. The dark $^1n_S\pi^*$ excited states of all SH-tautomers (E1, E3, E4) have higher vertical energies and the low-lying dark state is the $^1n_O\pi^*$ excited state. In the experimental UV spectra of the non-irradiated and irradiated samples of TBA we did not find any bands corresponding to the dark states which were calculated.

4. 3. Vibration Analysis of the Reactant and the Photoproducts

The experimental IR spectrum of TBA (KBr disc) has been reported by Mendez.[6] Unfortunately, the spectrum is rather structureless and featureless at the large and medium wavenumbers. Nevertheless, it is fairly informative with respect to the bands of the tautomers which Mendez has described.[6] The band assignment has shown that TBA exists in two tautomeric forms – tautomer K and tautomer E2. We registered the IR spectra of the irradiated and non-irradiated TBA, whose selected bands are compared in Fig. 2. The presented cuts comprise the most informative bands distinguishing the tautomers of TBA. Their frequencies (theoretical and experimental) are listed in Table 3.

The theoretically calculated frequencies were used to assign accurately the experimental bands which are fairly identical with those reported by Mendez for solid TBA.[6] For non-irradiated TBA, the most intensive band at

Table 3. Calculated and experimental (KBr disc) characteristic stretching vibrations of tautomeric forms of thiobarbituric acid

K				E			
Assign.	**Theoretical**		**Exp.**	**Assign.**	**Theoretical**		**Exp.**
	non scaled	**scaled***			**non scaled**	**scaled**	
ν_sNH	3580 / 32** /120***	3354	3234	νOH	3708 / 85 / 133	3469	3346–3666
ν_{as}NH	3576 / 8 / 107	–	–	νNH	3571 / 54 / 68	3346	3192–3086
$\nu_{as}CH_2$	3104 / 1 / 72	2926	3109	$\nu_{as}CH_2$	3094 / 0 / 98	2917	2928
ν_sCH_2	3068 / 6 / 2	2894	2876	ν_sCH_2	3059 / 0 / 276	2886	2862
ν_sC=O	1792 / 364 / 83	1747	1722	νC=O	1777 / 551 / 45	1733	1708
ν_{as}C=O	1772 / 603 / 41	1729	1682	νC=N	1671 / 634 / 157	1638	1686
νC=S	1539 / 560 / 50	1519	1566	νC=S	1473 / 233 / 73	1460	1531
ν_{as}NCN	1429 / 207 / 13	1421	1398	νC–O	1444 / 149 / 1	1434	1381
νC=S	1143 / 179 / 28	1163	1165	νC=S	1150 / 357 / 67	1170	1156
E1				**E2**			
νNH	3575 / 60 / 80	3349		νOH	3807 / 122 / 122	3558	3418–3564
$\nu_{as}CH_2$	3104 / 1 / 63	2926		ν_sNH	3606 / 89 / 66	3377	3234
ν_sCH_2	3066 / 1 / 149	2892		ν_{as}NH	3590 / 78 41	3363	–
νSH	2674 / 11 / 108	2540		νCH	3237 / 4 / 100	3046	2876
ν_sC=O	1795 / 321 / 52	1749		νC=O	1756 / 695 / 59	1714	1699
ν_{as}C=O	1767 / 317 / 47	1724		νC=C	1681 / 376 / 43	1647	1616
νC=N	1608 / 823 / 55	1581		νC–O	1266 / 104 / 1	1274	–
νC–N	1217 / 82 / 14	1230		νC–N,C–O	1230 / 177 / 12	1242	1244
νC–S	995 / 63 / 1	1030		νC=S	1145 / 202 / 7	1165	1165
E3				**E4**			
νOH	3708 / 79 / 155	3469		νOH	3807 / 106 / 122	3558	
$\nu_{as}CH_2$	3095 / 0 / 79	2918		νNH	3610 / 93 / 74	3381	
ν_sCH_2	3058 / 1 / 192	2885		νCH	3216 / 3 / 119	3027	
νSH	2663 / 3 / 117	2530		νSH	2678 / 10 / 91	2543	
νC=O	1763 / 327 / 68	1721		νC=O	1734 / 343 / 52	1695	
νC=N	1677 / 648 / 23	1643		νC=C	1707 / 657 / 38	1670	
νC=N	1532 / 654 / 104	1513		νC=N	1607 / 412 / 9	1581	
νC–O	1450 / 100 / 9	1439		νC–O	1270 / 133 / 5	1278	
νC–S	1116 / 285 / 16	1139		νC–S	1140 / 11 / 3	1161	

* The scaled frequencies were found by the equation $\nu_{exp} = 8.899\nu_{theor} + 136.2$. ** IR intensity / *** Raman activity

3109 cm^{-1} in Fig. 2a was assigned to the CH_2 asymmetric stretching vibration. The low intensity and shallow band in the interval 3346–3666 cm^{-1} was referred to the OH stretching vibration in tautomer E2. The band at 3234 cm^{-1} was assigned to the symmetric NH stretchings in the tautomeric forms K and E2. The bands at 2926, 2894, and 2876 cm^{-1} were referred to the ν_{as} and ν_s CH_2 stretching vibrations in tautomer K, and the CH stretch of the tautomer E2. The characteristic C=O stretching vibrations of the tautomers K and E2 (Fig. 2b, Table 3) were recorded at 1722 (K, ν_s), 1682 (K, ν_{as}), and 1699 cm^{-1} (E2). The C=S stretchings in the two forms were registered under 1600 cm^{-1}: the characteristic band at 1566 cm^{-1}, which is an indication that the thione form prevails in the solid state. The intensive band at 1165 cm^{-1} is also a proof in this aspect.

The comparisons of the theoretical and experimental stretching vibrations of the tautomer K led to the following correlation equation, $\nu_{exp} = 8.899\nu_{theor} + 136.2$, with a correlation coefficient of 0.989. This equation was used to scale the theoretical frequencies of all enol and thienol tautomers (see Table 3). The value of the correlation coefficient confirms the high accuracy of the B3LYP method for the prediction of the harmonic vibration frequencies of organic compounds.

The irradiated TBA shows a broad band in the interval 3192–3086 cm^{-1} which was assigned to the NH stretching vibration of the tautomer E. This band has a clear shoulder in the interval 3346–3666 cm^{-1} which comes from the OH stretching of the same tautomer. The broadening of the OH and NH bands indicates that the enol tautomer E forms H-bonds, inter- or intramolecular. Irradiated TBA shows bands at 2928 and 2862 cm^{-1} assigned to the asymmetric and symmetric CH_2 stretching vibrations. This is an indication that the CH_2 group was not affected by the UV-irradiation. This finding excludes tautomers E2 and E4 as photoproducts in the final photomixture. The calculations showed that all thienol tautomers should have a band for the S–H stretching vibration at about 2500 cm^{-1}. In the experimental IR spectra of irradiated and non-

irradiated TBA such characteristic band was not registered.

The IR spectrum of the irradiated TBA comprising the interval 1900–1000 cm^{-1} is presented in Fig. 2b. The bands at 1708 and 1686 cm^{-1} were assigned to the C=O and C=N stretching vibrations of the tautomer E. The C=S bands were recorded at 1531 and 1156 cm^{-1}, respectively. The band at 1381 cm^{-1} assigned to the C–O single-bond stretching vibration is an indication for the presence of an OH group in the photoproduct. The band at 1273 cm^{-1} (in the non-irradiated and irradiated spectra) was assigned, in agreement to Mendez,[6] to the CH in plane bending vibration in tautomer K. In the irradiated TBA this band has low intensity, which means that tautomer K dips out in the course of the UV-irradiation.

The analysis of the vibration spectra of the two samples (irradiated and non-irradiated) showed that the main photoproduct of the TBA should be the tautomer E. In other words, the UV-irradiation of TBA leads to the proton migration from the N-atom to the O-atom of one of the carbonyl groups. The second carbonyl group and N–H bond of TBA remain non-affected by the UV-light.

4. 4. Excited-State Reaction Paths

In order to explain the PIDA mechanism in TBA we studied the excited-state reaction paths of the NH dissociation in the tautomer K and the OH dissociation in the tautomer E. We believe that these processes are directly involved in the photoinduced keto-enol tautomerism of TBA. The excited state reaction paths are illustrated in Fig. 3. In both cases, the relative energies (E_{rel}) were determined by the energies of the ground-state equilibrium geometries of the tautomers K and E, respectively.

Fig. 3a illustrates the excited-state reaction paths of the H-detachment process in the tautomer K. The energy path of the ground state clearly shows the minimum of the ground state found at the N_1–H_{10} distance of 1.015 Å. The excited-state reaction paths of the low-lying $^1\pi\pi^*$ excited state and the second $^1\pi\pi^*$ excited state show crossings with the excited-state reaction paths of the bright $^1n_S\sigma^*$ and the repulsive $^1\pi\sigma^*$ excited state via conical intersections. In other words, the proton detachment process is driven by the bright $^1n_S\sigma^*$ excited state than by the repulsive $^1\pi\sigma^*$ excited state. Furthermore, the second $^1\pi\pi^*$ excited state plays much more pronounced role for the NH dissociation than the low-lying $^1\pi\pi^*$ excited state. The reason is that the system delivery from the second $^1\pi\pi^*$ excited state to the bright $^1n_S\sigma^*$ excited state passes through much lower energy barrier than the low-lying $^1\pi\pi^*$ excited state. The excited-state reaction path of the $^1n_S\sigma^*$ excited state leads to a low-lying conical intersection S_o–S_1 which mediate the radiationless relaxation of the excited system. The population of the low-lying $^1n_S\pi^*$ and $^1n_O\pi^*$ excited states, in the Franck–Condon region of the tautomer K, can be achieved via internal conversions through conical intersections with the excited-state reaction paths of the $^1n_S\sigma^*$ excited state. This population would lead to weak bands in the experimental fluorescent spectrum of TBA.

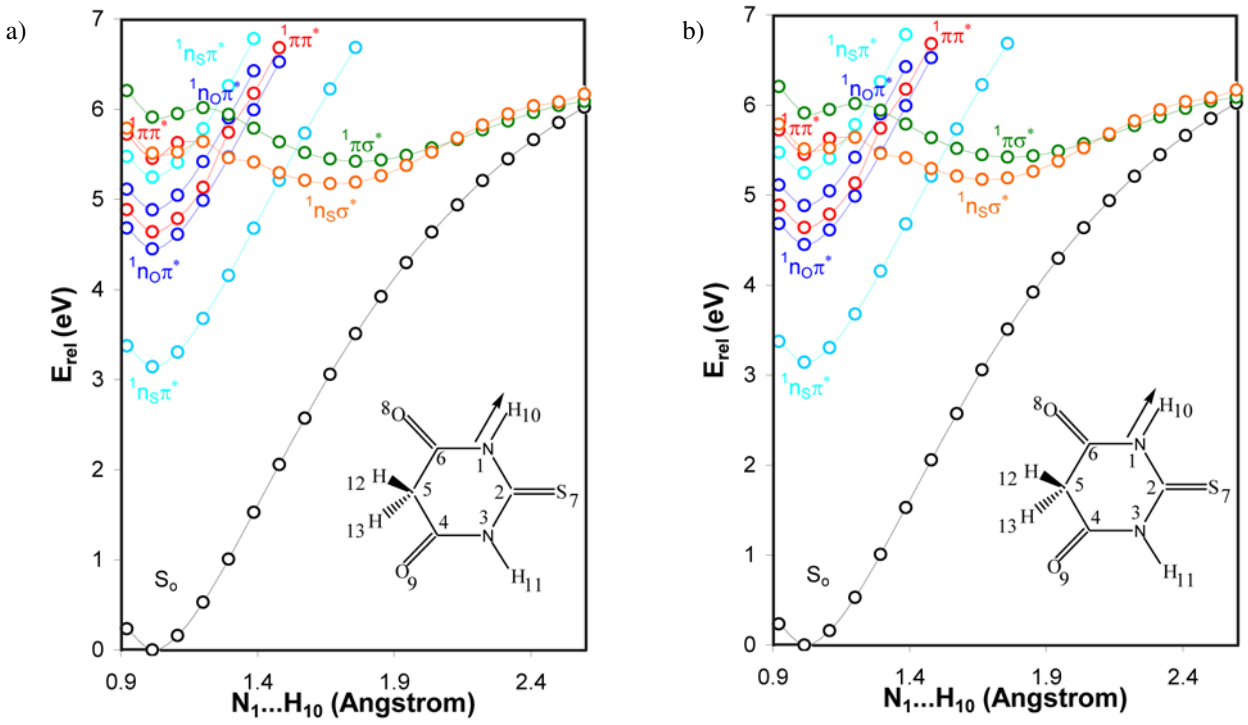

Figure 3. Excited-state reaction paths of the (a) NH dissociation process of the tautomer K, and (b) OH dissociation process of the tautomer E.

The excited-state reaction paths of the $^1n_S\sigma^*$ and $^1\pi\sigma^*$ excited states show minima at about N_1–H_{10} = 1.666 Å.

In Fig. 3b are depicted the excited-state reaction paths for the OH dissociation of the tautomer E. These curves are similar to the energy profiles shown in Fig. 3a. However, there is one significant exception: the excited-state reaction path of the $^1n_S\sigma^*$ excited state does not lead to a low-lying S_o–S_1 conical intersection (or a crossing with the ground-state reaction path). A crossing exists between the reaction paths of the $^1\pi\sigma^*$ excited state and the S_o state. It defines a low-lying conical intersection of the type S_o–S_1. Such crossing is usually observed in pyrimidine bases.[14] Since the repulsive $^1\pi\sigma^*$ excited state is a dark state, the OH dissociation of the tautomer E would occur not as easy as the NH dissociation of the tautomer K. Furthermore, the tautomer K was found to be the most stable form of TBA which means that the irradiation of TBA with UV light would lead to the accumulation of the tautomer E in the final photomixture. The excited-state reaction paths of the $^1\pi\sigma^*$ and $^1n_S\sigma^*$ excited states show minima at the N_1–H_{10} distance of 1.624 Å. The minima are deeper than those of the NH dissociation of the tautomer K. Comparing the ground state minima in Fig. 3 one can see that the minimum of the tautomer E is much deeper than the minimum of the tautomer K. It means, that the second order Jahn–Teller effect should be observed in a greater extent in the tautomer K than in the tautomer E.

5. Conclusion

We performed a combined, theoretical and experimental, study of the photoinduced tautomerism of TBA. In agreement with previous investigations,[6,10] our study showed that the triketo tautomer of TBA is predominant in the solid state. The UV-irradiation of TBA leads to the accumulation of the hydroxy-imino tautomer E as the major photoproduct. The theoretical calculations performed at the TD DFT level showed that the tautomer K transforms photochemically into tautomer E via low-lying S_o–S_1 conical intersection(s). This process predominantly occurs in the bright $^1n_S\sigma^*$ excited state. This state of the tautomer K can be populated from the second $^1\pi\pi^*$ excited state through internal conversion and an appropriate conical intersection. The photochemical OH dissociation of the tautomer E is driven by the repulsive $^1\pi\sigma^*$ excited state.

6. Acknowledgements

We thank Mrs. Neda Danova, Dr. Plamen Penchev, and Dr. Maria Stoyanova from the Chemical faculty of the University of Plovdiv for the recording of the UV and IR spectra. We also thank the National Science Fund of Bulgaria, Project RNF01/0110, and the Science Fund of the University of Plovdiv, RNI 09-HF-002, for the support.

7. References

1. F. Zuccarello, G. Buemi, C. Gandolfo, A. Contino, *Spectrochim. Acta Part A* **2003**, *59*, 139–151.
2. A. Gringauz, in: Introduction to Medicinal Chemistry – How Drugs Act and Why, Wiley-VCH, New York, **1997**.
3. S. R. Marder, D. N. Beratan, L.-T. Cheng, *Science* **1991**, *252*, 103–106.
4. (*a*) S. R. Marder, L.-T. Cheng, B. G. Tiemann, A. C. Friedli, M. Blanchard-Desce, J. W. Perry, J. Skindhøj, *Science* **1994**, *263*, 511–514.; (*b*) M. Blanchard-Desce, V. Alain, P. V. Bedworth, S. R. Marder, A. Fort, C. Runser, M. Barzoukas, S. Lebus, R. Wortmann, *Chem. Eur. J.* **1997**, *3*, 1091–1104.
5. J. Adamson, B. J. Coe, H. L. Grassam, J. C. Jeffery, S. J. Coles, M. B. Hursthouse, *J. Chem. Soc., Perkin Trans.* **1999**, *1*, 2483–2488.
6. E. Mendez, M. F. Cerda, J. S. Gancheff, J. Torres, C. Kremer, J. Castiglioni, M. Keininger, O. N. Ventura, *J. Phys. Chem. C* **2007**, *111*, 3369–3383.
7. M. R. Chierotti, L. Ferrero, N. Garino, R. Gobetto,L. Pellegrino, D. Braga, F. Grepioni,L. Maini, *Chem. Eur. J.* **2010**, *16*, 4347–4358.
8. R. K. Goel, C. Gupta, S. P. Gupta, *Ind. J. Pure. Appl. Chem.* **1985**, *23*, 344–350.
9. M. S. G. Tasende, M. I. S. Gimeno, S. Sanchez, J. S. Casas, J. Sordo, *J. Organomet. Chem.* **1990**, *390*, 293–300.
10. S. Millefiori, A. Millefiori, *J. Heterocyclic Chem.* **1989**, *26*, 639–644.
11. R. Martos-Calvente,V. A. de la Pena O'Shea, J. M. Campos-Martin, J. L. G. Fierro, *J. Phys. Chem. A* **2003**, *107*, 7490–7495.
12. B. Chmura, M. Rode, A. Sobolewski, L. Lapinski, M. Nowak, *J. Phys. Chem. A* **2008**, *112*, 13655–13661.
13. A. L. Sobolewski, *Chem. Phys. Lett.* **1993**, *211*, 293–299.
14. V. B. Delchev, A. L. Sobolewski, W. Domcke, *Phys. Chem. Chem. Phys.* **2010**, *12*, 5007–5015.
15. T. H. Dunning, Jr., *J. Chem. Phys.* **1989**, *90*, 1007–1014.
16. R. A. Kendall, T. H. Dunning, Jr., R. J. Harrison, *J. Chem. Phys.* **1992**, *96*, 6796–6807.
17. Gaussian 03, Revision D.01, M. J. Frisch, G. W. Trucks, H. B. Schlegel, G. E. Scuseria, M. A. Robb, J. R. Cheeseman, J. A. Montgomery, Jr., T. Vreven, K. N. Kudin, J. C. Burant, J. M. Millam, S. S. Iyengar, J. Tomasi, V. Barone, B. Mennucci, M. Cossi, G. Scalmani, N. Rega, G. A. Petersson, H. Nakatsuji, M. Hada, M. Ehara, K. Toyota, R. Fukuda, J. Hasegawa, M. Ishida, T. Nakajima, Y. Honda, O. Kitao, H. Nakai, M. Klene, X. Li, J. E. Knox, H. P. Hratchian, J. B. Cross, V. Bakken, C. Adamo, J. Jaramillo, R. Gomperts, R. E. Stratmann, O. Yazyev, A. J. Austin, R. Cammi, C. Pomelli, J. W. Ochterski, P. Y. Ayala, K. Morokuma, G. A. Voth, P. Salvador, J. J. Dannenberg, V. G. Zakrzewski, S. Dapprich, A. D. Daniels, M. C. Strain, O. Farkas, D. K. Malick, A. D. Rabuck, K. Raghavachari, J. B. Foresman, J. V. Ortiz, Q. Cui, A. G. Baboul, S. Clifford, J. Cioslowski, B. B. Stefanov, G. Liu, A. Liashenko, P. Piskorz, I. Komaromi, R. L. Martin, D. J. Fox, T. Keith, M. A. Al-Laham, C. Y. Peng, A. Nanayakka-

ra, M. Challacombe, P. M. W. Gill, B. Johnson, W. Chen, M. W. Wong, C. Gonzalez, and J. A. Pople, Gaussian, Inc., Wallingford CT, 2004.

18. R. Ahlrichs, M. Baer, M. Haeser, H. Horn, C. Koelmel, *Chem. Phys. Lett*. **1989**, *162*, 165–169.
19. C. Haettig, F. Weigend, *J. Chem. Phys.* **2000**, *113*, 5154–5162.

Povzetek

Predstavljamo teoretične in eksperimentalne raziskave, ki so nam omogočile študij mehanizma fotoinducirane tavtomerije 2-tiobarbiturne kisline (TBA). Obsevanje raztopine TBA v polarnem aprotičnem topilu z UV svetlobo (z maksimumom pri 366 nm) je pokazalo, da poteče okso-hidroksi fotoizomerizacija iz triketo oblike TBA v hidroksi-iminski tavtomer. Študij mehanizma (TD DFT) fotoinducirane disociacije NH in OH v keto in enolnem tavtomeru je pokazal, da odcep protona iz triketo tavtomera poteka preko svetlega $^1n_S\sigma^*$ vzbujenega stanja; v hidroksi-iminskem tavtomeru pa je mehanizem gnan z odbojnim $^1\pi\sigma^*$ vzbujenim stanjem. Relaksacija vzbujenega stanja poteka preko nizko energijskega S_o–S_1 koničnega presečišča.

Electronic supporting information

Photoinduced Tautomerism of 2-thiobarbituric Acid Studied by Theoretical and Experimental Methods

R. Bakalska and V. B. Delchev

Table S1. Calculated CC2 vertical excitation energies of the tautomeric forms of thiobarbituric acid

K			**E**		
	eV	**nm**		**eV**	**nm**
$^1n_S\pi^*$ (A")	3.489	356	$^1n_S\pi^*$ (A")	2.842	437
$^1n_O\pi^*$ (A")	4.728	262	$^1\pi\pi^*$ (A')	4.489	276
$^1\pi\pi^*$ (A')	4.729	262	$^1n_O\pi^*$ (A")	4.747	261
$^1n_O\pi^*$ (A")	5.081	244	$^1n_N\pi^*$ (A")	5.083	244
$^1n_S\pi^*$ (A")	6.272	198	$^1n_S\pi^*$ (A")	5.651	220
$^1\pi\pi^*$ (A')	5.586	222	$^1n_S\sigma^*$ (A')	5.573	223
$^1n_S\sigma^*$ (A')	5.822	213	$^1\pi\pi^*$ (A')	5.345	232
$^1\pi\pi^*$ (A')	6.726	184	$^1\pi\pi^*$ (A')	6.245	199
$^1\pi\sigma^*$ (A")	6.208	200	$^1n_S\sigma^*$ (A')	6.393	194
E1			**E2**		
$^1n_O\pi^*$ (A")	3.833	324	$^1n_S\pi^*$ (A")	3.932	316
$^1\sigma\pi^*$ (A")	4.828	257	$^1n_S\pi^*$ (A")	5.744	216
$^1\pi\pi^*$ (A')	5.076	244	$^1\pi\pi^*$ (A')	4.680	265
$^1n_N\pi^*$ (A")	5.193	239	$^1\pi\pi^*$ (A')	5.084	244
$^1\pi\pi^*$ (A')	5.794	214	$^1\pi\sigma^*$ (A")	5.439	228
$^1\pi\sigma^*$ (A")	5.866	212	$^1n_S\sigma^*$ (A')	5.675	219
$^1n_O\sigma^*$ (A')	5.905	210	$^1n_O\pi^*$ (A")	4.991	249
$^1n_O\pi^*$ (A")	6.185	201	$^1\pi\pi^*$ (A')	5.592	222
$^1n_O\sigma^*$ (A')	6.353	195	$^1n_O\pi^*$ (A")	5.552	234
E3			**E4**		
$^1n_O\pi^*$ (A")	3.543	350	$^1n_O\pi^*$ (A")	4.441	279
$^1n_N\pi^*$ (A")	4.340	286	$^1n_O\pi^*$ (A")	4.773	260
$^1\pi\pi^*$ (A')	4.533	274	$^1\pi\pi^*$ (A')	5.129	242
$^1\pi\pi^*$ (A')	5.342	232	$^1\pi\sigma^*$ (A")	5.396	230
$^1n_N\pi^*$ (A")	5.724	217	$^1n_O\sigma^*$ (A')	5.251	236
$^1n_O\pi^*$ (A")	5.652	220	$^1\pi\sigma^*$ (A")	5.633	220
$^1\pi\sigma^*$ (A")	6.203	200	$^1\pi\sigma^*$ (A")	5.826	213
$^1n_O\sigma^*$ (A')	5.893	211	$^1n_O\sigma^*$ (A')	5.634	220
$^1\pi\pi^*$ (A')	6.780	183	$^1\pi\pi^*$ (A')	5.735	216

Table S2. Adiabatic excitation energies (CC2) of the tautomeric forms of thiobarbituric acid

Optimized		**K**			**E**			**E1**	
state	**State**	**eV**	**nm**	**State**	**eV**	**nm**	**State**	**eV**	**nm**
$^1\pi\pi^*$ (A')	$^1n_S\pi^*$	2.730	455	Cannot be optimized			$^1n_O\pi^*$	1.822	681
	$^1\pi\pi^*$	3.390	366				$^1\pi\pi^*$	2.817	441
	$^1n_O\pi^*$	4.511	275				$^1\sigma\pi^*$	3.907	318
	$^1\sigma\pi^*$	4.880	254				$^1n_O\sigma^*$	4.041	307
$^1n_S\pi^*$ (A'')	$^1n_S\pi^*$	3.023	410	$^1n_S\pi^*$	2.075	598	$^1n_O\pi^*$	1.335	930
for K and E	$^1\pi\pi^*$	4.097	303	$^1\pi\pi^*$	3.487	356	$^1\pi\pi^*$	3.158	393
$^1n_O\pi^*$ (A'')	$^1n_O\pi^*$	4.500	276	$^1\sigma\pi^*$	4.409	281	$^1n_O\sigma^*$	3.573	347
for E1	$^1\sigma\pi^*$	4.927	252	$^1n_O\pi^*$	4.848	256	$^1n_O\pi^*$	3.901	318
		E2			**E3**			**E4**	
$^1\pi\pi^*$ (A')	$^1n_S\pi^*$	3.186	389	$^1n_O\pi^*$	1.610	771	$^1n_O\pi^*$	1.270	977
	$^1\pi\pi^*$	3.673	338	$^1\pi\pi^*$	2.189	567	$^1\pi\pi^*$	2.284	543
	$^1\pi\pi^*$	4.779	260	$^1n_N\pi^*$	2.876	431	$^1n_O\sigma^*$	2.839	437
	$^1n_S\pi^*$	4.818	258	$^1n_O\pi^*$	4.490	276	$^1n_O\pi^*$	2.878	431
$^1n_S\pi^*$ (A'')	$^1n_S\pi^*$	3.345	371	$^1n_O\pi^*$	0.725	1712	$^1n_O\pi^*$	1.178	1053
for E2	$^1\pi\pi^*$	4.057	306	$^1\pi\pi^*$	2.176	570	$^1\pi\pi^*$	2.289	542
$^1n_O\pi^*$ (A'')	$^1n_O\pi^*$	4.870	255	$^1\sigma\pi^*$	3.087	402	$^1n_O\pi^*$	2.679	463
for E3 and E4	$^1\pi\pi^*$	4.900	253	$^1n_O\sigma^*$	3.521	352	$^1n_O\sigma^*$	2.691	461

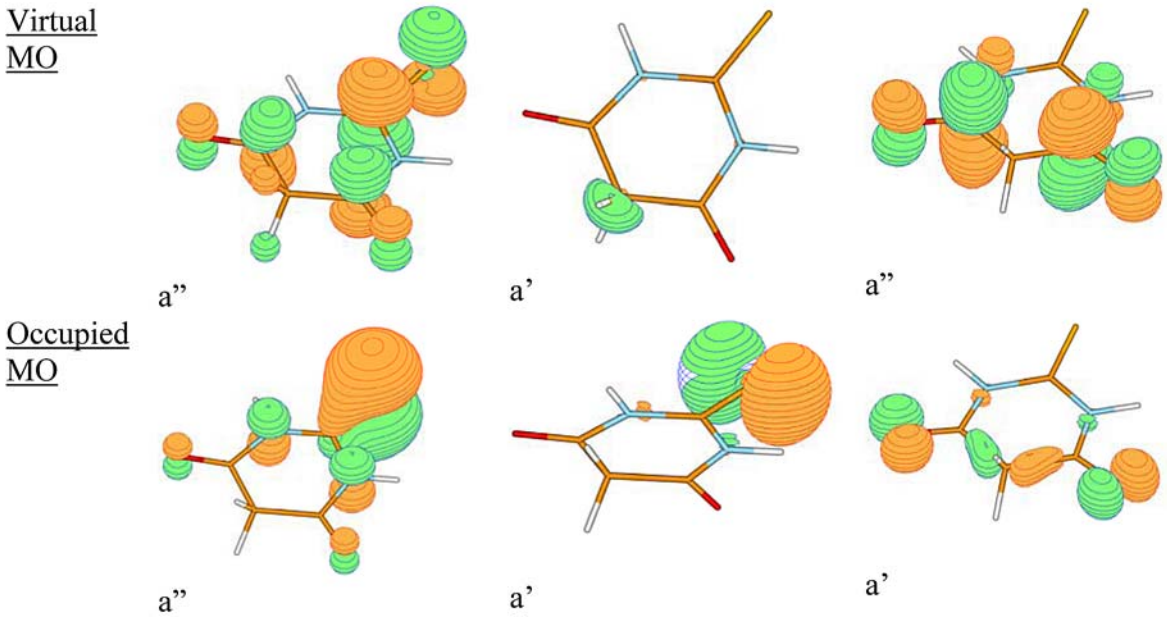

Figurs S1. Selected molecular orbitals (optimized at the CC2 level) of the oxo form (K) of TBA involved in the electron transitions

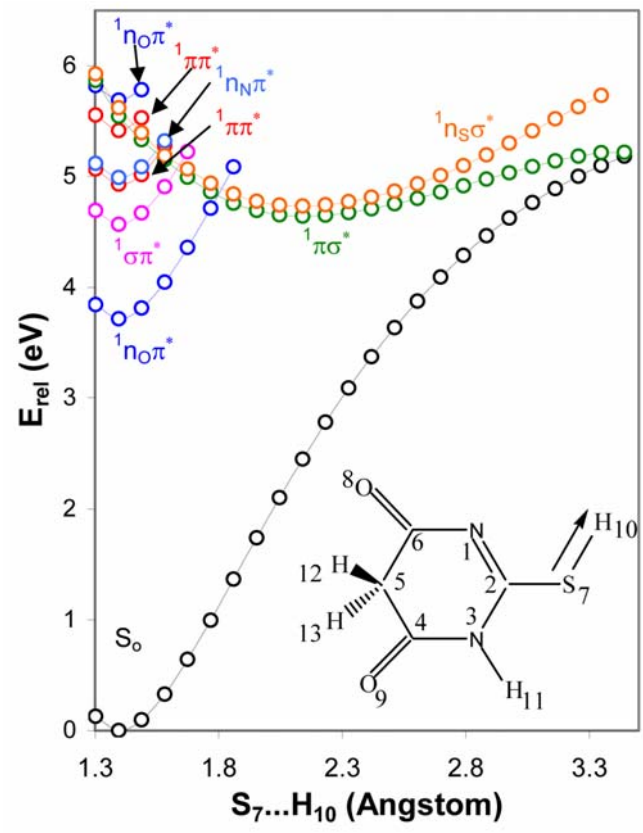
$^1n_O\pi^*$
$^1\pi\pi^*$
$^1n_N\pi^*$
$^1\pi\pi^*$
$^1n_S\sigma^*$
$^1\sigma\pi^*$
$^1\pi\sigma^*$
$^1n_O\pi^*$
S_o
E_{rel} (eV)
$S_7...H_{10}$ (Angstom)
8O
6
N
1
12 H
5
2
S_7
H_{10}
13 H
4
3
N
O 9
H_{11}

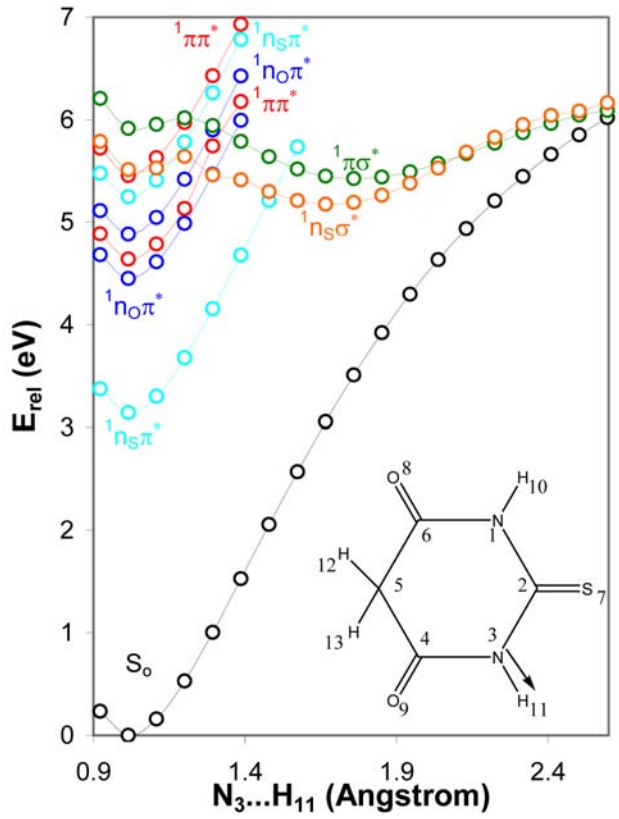
$^1\pi\pi^*$
$^1n_S\pi^*$
$^1n_O\pi^*$
$^1\pi\pi^*$
$^1\pi\sigma^*$
$^1n_S\sigma^*$
$^1n_O\pi^*$
$^1n_S\pi^*$
S_o
E_{rel} (eV)
$N_3...H_{11}$ (Angstrom)
O 8
H_{10}
6
N
1
12 H
5
2
S_7
13 H
4
3
N
O 9
H_{11}